International Journal of Pharmaceutical Science Invention
ISSN (Online): 2319-6718, ISSN (Print): 2319- 670X
www.ijpsi.org Volume 14 Issue 3 ǁ May –June, 2025 ǁ PP. 156-166

In Silico Screening of Hericium Genus Metabolites Against Beta-Secretase: A Therapeutic Insight into Alzheimer's Disease.

Dr. Veeresh. B[1], S. Apoorva [1], Gunte Pranai [2], Boorgu Durga Prasad [2,]
[1&2] *Department of Pharmacology G. Pulla Reddy college of Pharmacy, Osmania University, India.*

ABSTRACT
Computer-aided drug design (CADD) quickens the progress of new therapies by using in silico modelling to identify potential neuroprotective agents. Studying erinacines S, A, and C as potential Alzheimer's disease (AD) treatments, we explore the potential of natural bioactive compounds from the mushroom genus Hericium. Erinacine S appears to lessen the buildup of amyloid-beta (Aβ) plaques by boosting nerve growth factor (NGF) levels and crossing the blood-brain barrier. Erinacine C helps regulate glial-derived neurotrophins and displays anti-inflammatory effects in the brain, while erinacine A activates neurotrophic signalling pathways and promotes the growth of new neurons in the hippocampus. In addition, we examine novel compounds that may help counteract endoplasmic reticulum (ER) stress and restore estrogen receptor function—both of which are disrupted in AD. In particular, the dysfunction of estrogen receptor alpha (erα) and the increased activity of beta-secretase (BACE1) are highlighted as key contributors to disease progression. Through molecular docking studies, we evaluate how Hericium-derived compounds interact with BACE1, suggesting a promising natural product-based approach to developing new therapies for Alzheimer's disease.

Date of Submission: 15-06-2025 Date of acceptance: 30-06-2025

I. INTRODUCTION:

A particularly successful strategy for drug development and discovery is computer-aided drug design. It allows us swiftly and economically identify the most promising medication candidate. We can lessen our efforts at biological and synthetic testing by using it. By using in silico filters to remove molecules with undesired qualities (low effectiveness, weak ADMET, etc.), it yields the most promising therapeutic candidate. It is a quick, automated, time-saving, and cost-effective procedure. It allows us to learn about the pattern of drug-receptor interactions [1].

Compound **Erinacine S ($C_{25}H_{34}O_6$)** have been found to pass the blood-brain barrier in rats. This capacity to traverse the blood-brain barrier allows these chemicals to increase NGF production in the brain, overcoming the constraints of NGF, which cannot efficiently pass the blood-brain barrier [2]. and also lessen the quantity and size of Ab plaques in an Alzheimer's disease mice model (APP/PS1). Additionally, it encourages the buildup of neurosteroids, which are known to stimulate neurogenesis, reduce neuronal death, and encourage neurite outgrowth. The neuroprotective effects of erinacine S on Alzheimer's disease and neuronal regeneration are explained by this buildup of neurosteroids [3]. **Compounds $C_9H_{11}ClO_2$ and $C_9H_9ClO_3$** have been explored for their ability to inhibit endoplasmic reticulum stress which submits they also wield neuroprotective effects [2]. It has been reported that **erinacine A ($C_{26}H_{38}O_6$)** exerts its neuroprotective and neurotrophic activities through multiple signaling pathways. Activating the TrkA/Erk1/2 pathway is one of the mechanisms by which erinacine A ($C_{26}H_{38}O_6$) promotes PC12 cell survival and differentiation. In a mouse model of AD, administration of erinacine A ($C_{26}H_{38}O_6$) inhibited the formation of Aβ and reduced plaque accumulation in the brain. In vivo experiments demonstrated that erinacine A ($C_{26}H_{38}O_6$) decreased cortical size, inhibited the growth of amyloid plaques in the hippocampal region, and promoted hippocampal neurogenesis [2]. In rats, erinacine A ($C_{26}H_{38}O_6$) effectively increased the amount of NGF in the hippocampus and locus coeruleus [4]. **Erinacine C($C_{25}H_{38}O_6$)** causes glial cells to express BDNF and NGF. The resulting NGF can then set off a series of signals that cause PC12 cells to differentiate, or begin to take on the characteristics of more specialized neurons. Erinacine C($C_{25}H_{38}O_6$) is essential for controlling proliferation and regeneration in the central nervous system because it stimulates E26 transformation-specific (ETS)-dependent transcription in astrocytes, regardless of the mechanism by which it causes PC12 cell differentiation [2]. In BV2 microglial cells, erinacine C ($C_{25}H_{38}O_6$) protects against neuroinflammation by preventing NO, IL-6, and TNF-secretion as well as inhibition of NF-Band phosphorylation of IB [5]. **Raloxifene ($C_{28}H_{27}NO_4S$)** is the first Selective Estrogen Receptor Modulator (SERM) approved for the prevention and treatment of osteoporosis in postmenopausal women [6]. Since hormonal changes during

menopause may have an impact on the pathophysiology of AD, Raloxifene ($C_{28}H_{27}NO_4S$) shows promise in preventing AD in postmenopausal women [7]. Mild cognitive impairment can be prevented and restored with raloxifene [8].

In Alzheimer's disease (AD), aberrant clusters of tau protein in the brain called neurofibrillary tangles (NFTs) contain the estrogen receptor alpha (ERα). This indicates that ERα becomes entangled in these tangles. ERα is unable to carry out its function, which involves using estrogen signaling to protect brain cells, when it is trapped in NFTs [9]. ERα exerts neuroprotection against AD by maintaining intracellular signaling cascades and the study reported reduced expression of ERα in hippocampal neurons of AD patients [10]. The idea that BACE1 is essential to AD pathophysiology is supported by the observation that BACE1 concentrations and activity rates are elevated in AD brains and bodily fluids. Consequently, BACE1 is a prime target for drugs that slow down the generation of Aβ [11].

TABLE:1

S.NO	MOLECULAR FORMULA	STRUCTURE
1.	$C_{25}H_{34}O_6$	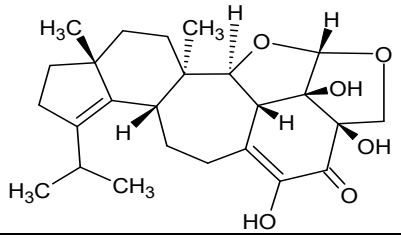
2.	$C_9H_{11}ClO_2$	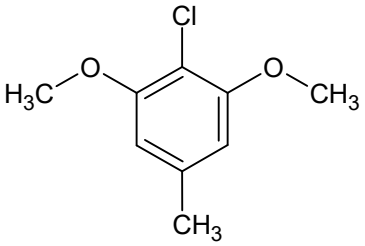
3.	$C_9H_9ClO_3$	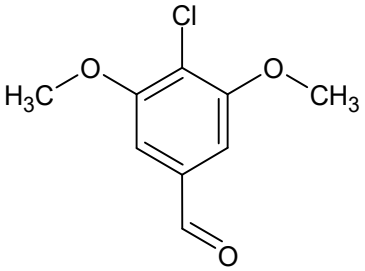
4.	$C_{26}H_{38}O_6$	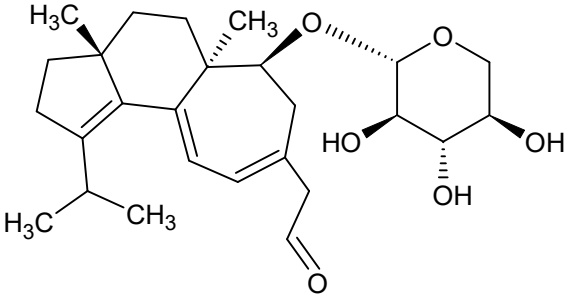
5.	$C_{25}H_{38}O_6$	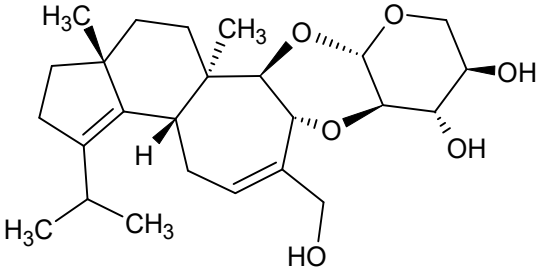

6.	$C_{28}H_{27}NO_4S$ (standard)	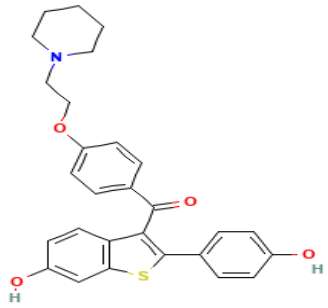

II. MOLECULAR DOCKING:

One computer method utilized in drug discovery and other biomolecular research domains is molecular docking. It promotes the contact between a larger biomolecule (receptor), like a protein, and a smaller molecule (ligand). The program examines the ligand's position and conformation as it attaches to the receptor's active site. For molecular docking, there are a number of software programs available, each with its own strengths and weaknesses. Some examples are Auto Dock, Auto Dock Vina, and so on. By assisting in the identification of possible lead compounds that might have advantageous binding interactions with a target molecule, these technologies are essential in the early phases of drug discovery.

III. MATERIALS:

The most dependable ways to begin a research process were determined to be computational approaches. As a result, a number of computational tools that could be used to produce novel molecules efficiently may be based on ongoing research. Web tools were used to study the created derivatives in order to comprehend their biological activities, physicochemical characteristics, and potential toxicological impacts.

TABLE:2

S.NO	MATERIALS	METHODOLOGY
1	Chemsketch	Generation of ligand structures
2	Molinspiration	Molecular property prediction
3	Swiss ADME	Prediction of pharmacokinetic properties
4	PASS studies	Prediction of biological activity
5	GUSAR	Toxicological studies
6	Autodock vina 1.5.7	Molecular docking
7	Biovia Discovery studio 2021	Visualization of interactions

IV. METHODOLOGY:

4.1 Prediction of physicochemical and ADMET properties: When developing new drugs, ADMET qualities are essential. In addition to having adequate efficacy, a successful drug candidate must also have the right ADMET characteristics. In order to estimate ADMET qualities, computer simulation techniques are now being developed. Throughout the whole drug design, discovery, and development process, these characteristics of chemical entities are dynamic. Finding effective therapeutic compounds with enhanced ADME characteristics is therefore likely.

4.2 Molinspiration: Molinspiration is a web-based tool that facilitates standardization of molecules, translation of SMILES and SDfiles, and molecular administration and processing. Higher quality molecule portrayal, molecular database tools, auxiliary substructure and resemblance searches, tautomer creation, molecular fragmentation, computation of many molecular attributes desired in QSAR research, molecular modeling and innovative drug design, and more. Likewise, bioactivity screening, visualization, and fragment-based virtual screening are provided. In addition to estimating the bioactivity score for the most important drug targets (GPCR ligands, ion channel modulators, kinase inhibitors, nuclear receptors), molinspiration web tools are used to calculate important molecular properties (polar surface area, log P, number of hydrogen bond acceptors and donors, and others). This web tool predicts the physicochemical properties.

4.3 swissADME: In order to support novel drug discovery, swissADME enables us to forecast ADMET properties, pharmacokinetic parameters, drug likeness, and medicinal chemistry approachability of one or several small molecules. The computer-based studies include not only lead generation, hit optimization, binding energy

calculation, interaction design determination of the minor molecules to the enzyme pouch, and dynamic recreation studies, but also the estimation of physicochemical properties and pharmacokinetic properties of the trivial new molecules. Various tools can be hired for the same purpose, but swissADME is a popular web tool because it is free to use.

V. Molecular Docking Studies:

During the drug development process, computational techniques are equally necessary and advantageous resources. Planning, searching, evaluating, modeling, calculating binding energy, pharmacokinetic parameters and pharmacokinetic predictions, and the lead optimization process became considerably simpler with the advent of computer tools. One important online technique in structural biology and computer-aided drug creation is computational molecular docking. Predicting the principal binding model of a ligand molecule with a target protein of known three-dimensional molecular structure is the primary objective of ligand-target protein docking. In addition to employing a scoring system that will suitably rank candidate dockings, effective molecular docking techniques are employed to search high dimensional spaces with exceptional efficiency.

5.1 Steps involved in molecular docking:

Step-1: prepare the protein:

Protein preparation involves downloading the protein's structure from the open-source protein database. The structure is transformed to the pdbqt format and retained after the water molecules are eliminated, the bounded ligands are eliminated using auto dock vina software, polar hydrogen is added, and Kohlmann charges are introduced.

Step-2: prepare the ligands:

The ligands' 2-D structure is sketched, transformed into 3-D structure format using Chem Sketch, and stored in pdb format. Auto dock Vina program then converts the pdb into pdbqt format for the docking research.

Step-3: performing the docking:

AutoDock 1.4.7 was used for molecular docking. To identify the active binding site and how it interacts with ligand molecules, molecular docking studies were conducted. Since the active binding site for the newly synthesized chemical was unknown, blind docking tests were conducted in order to choose both the ligand and the macromolecule and achieve the rigid grid box using Auto-grid. Each target and ligand's grid box dimensions were then saved in a different file and recorded as a text document in the config file. A command prompt was used to forecast the binding scores of these ligand-target complexes. The path for the results and the intended syntax for the forecast were provided. As a result, the output file in the provided file contained the scores that were acquired. Interactions were examined using the docked output files. Biovia Discovery Studio was used to display the position with the highest binding affinity

Step-4: Visualization:

Ligand target Molecular complex visualization is a momentous aspect of the investigation and communication of modeling studies. It permits a mechanistic understanding of a molecular structure to be visualized. Protein and other tiny molecular data can be observed, allocated, and analyzed using the feature-rich, free web program BIOVIA Discovery Studio Visualizer. In order to visualize the active site and 2D interactions and determine which atom is bonding with which amino acid of the target molecule, the best scoring output among the nine conformers was used in Biovia Discovery Studio. This was done using the output files that were obtained for each ligand against each target separately. Complexes that were visualized were therefore saved as picture files.

VI. RESULTS AND DISCUSSION:

6.1 ADMET properties of compounds: We can determine whether a compound is suitable for use as a drug using Molinspiration.

TABLE:3

S.NO	FORMULA	MOL.WT	NHD	NHA	NRB	Log P	Violations
1.	$C_{25}H_{34}O_6$	430.53	3	6	1	2.85	0
2.	$C_9H_{11}ClO_2$	186.64	0	2	2	2.52	0
3.	$C_9H_9ClO_3$	200.62	0	3	3	1.99	0
4.	$C_{26}H_{38}O_6$	446.58	3	6	5	3.20	0
5.	$C_{25}H_{38}O_6$	434.57	3	6	2	3.50	0
6.	$C_{28}H_{27}NO_4S$ (standard)	473.58	2	5	7	3.76	0

6.2 Pharmacokinetic properties using swiss ADME:

By applying Swiss ADME for pharmacokinetic properties, we can determine the drug's "Log Kp" route of delivery. Skin permeability gauges the compound's ability to penetrate skin. A log kp value greater than -2.5 cm (about 0.98 in/s) denotes low skin permeability. The BBB permeability determine whether a medicine can pass the blood-brain barrier. Low GI absorption means the medication is not suitable for oral administration.

TABLE:4

S.NO	FORMULA	Log Kp cm/s	Gi abs	BBB Permeability	INHIBITORY INTERACTIONS					
					P-pg. substrate	CYP 1A2	CYP2 C19	CYP2 C9	CYP 2D6	CYP 3A4
1.	$C_{25}H_{34}O_6$	-7.58	High	No	Yes	No	No	No	No	No
2.	$C_9H_{11}ClO_2$	-5.41	High	Yes	No	Yes	No	No	No	No
3.	$C_9H_9ClO_3$	-6.07	High	Yes	No	Yes	No	No	No	No
4.	$C_{26}H_{38}O_6$	-7.80	High	No	Yes	No	No	No	No	No
5.	$C_{25}H_{38}O_6$	-7.94	High	No	Yes	No	No	No	No	No
6.	$C_{28}H_{27}NO_4S$	-4.86	High	No	Yes	No	Yes	No	Yes	No

6.3 Acute toxicity predicted by GUSAR:

GUSAR calculates the medication dosage. It uses the LD50 value to calculate the drug's fatal dose. The dose of medication administered all at once that will kill half of the subjects is known as the LD50. It protects against drug toxicity and guarantees safety.

TABLE:5

$C_{25}H_{34}O_6$	**Rat IP LD50 Log10(mmol/kg)** / **Rat IV LD50 log10(mmol/kg)** / **Rat Oral LD50 log10(mmol/kg)** / **Rat SC LD50 log10(mmol/kg)** -0,306 in AD / -1,630 in AD / 0,001 in AD / -1,502 in AD **Rat IP LD50 (mg/kg)** / **Rat IV LD50 (mg/kg)** / **Rat Oral LD50 (mg/kg)** / **Rat SC LD50 (mg/kg)** 213,000 in AD / 10,090 in AD / 431,300 in AD / 13,550 in AD **Acute Rodent Toxicity Classification of Chemicals by OECD Project** **Rat IP LD50 Classification** / **Rat IV LD50 Classification** / **Rat Oral LD50 Classification** / **Rat SC LD50 Classification** Class 4 in AD / Class 3 in AD / Class 4 in AD / Class 2 in AD
$C_9H_{11}ClO_2$	**Rat IP LD50 Log10(mmol/kg)** / **Rat IV LD50 log10(mmol/kg)** / **Rat Oral LD50 log10(mmol/kg)** / **Rat SC LD50 log10(mmol/kg)** 0,635 in AD / -0,767 in AD / 1,139 in AD / 0,860 in AD **Rat IP LD50 (mg/kg)** / **Rat IV LD50 (mg/kg)** / **Rat Oral LD50 (mg/kg)** / **Rat SC LD50 (mg/kg)** 804,900 in AD / 31,940 in AD / 2568,000 in AD / 1354,000 in AD **Acute Rodent Toxicity Classification of Chemicals by OECD Project** **Rat IP LD50 Classification** / **Rat IV LD50 Classification** / **Rat Oral LD50 Classification** / **Rat SC LD50 Classification** Class 5 in AD / Class 3 in AD / Class 5 in AD / Class 5 in AD
$C_9H_9ClO_3$	**Rat IP LD50 Log10(mmol/kg)** / **Rat IV LD50 log10(mmol/kg)** / **Rat Oral LD50 log10(mmol/kg)** / **Rat SC LD50 log10(mmol/kg)** 0,508 in AD / -0,666 in AD / 1,123 in AD / 1,058 in AD **Rat IP LD50 (mg/kg)** / **Rat IV LD50 (mg/kg)** / **Rat Oral LD50 (mg/kg)** / **Rat SC LD50 (mg/kg)** 646,700 in AD / 43,300 in AD / 2666,000 in AD / 2292,000 in AD **Acute Rodent Toxicity Classification of Chemicals by OECD Project** **Rat IP LD50 Classification** / **Rat IV LD50 Classification** / **Rat Oral LD50 Classification** / **Rat SC LD50 Classification** Class 5 in AD / Class 4 in AD / Class 5 in AD / Class 5 in AD
$C_{26}H_{38}O_6$	**Rat IP LD50 Log10(mmol/kg)** / **Rat IV LD50 log10(mmol/kg)** / **Rat Oral LD50 log10(mmol/kg)** / **Rat SC LD50 log10(mmol/kg)** -0,557 in AD / -1,468 in AD / 0,193 in AD / -0,992 in AD **Rat IP LD50 (mg/kg)** / **Rat IV LD50 (mg/kg)** / **Rat Oral LD50 (mg/kg)** / **Rat SC LD50 (mg/kg)** 123,900 in AD / 15,200 in AD / 697,000 in AD / 45,520 in AD **Acute Rodent Toxicity Classification of Chemicals by OECD Project** **Rat IP LD50 Classification** / **Rat IV LD50 Classification** / **Rat Oral LD50 Classification** / **Rat SC LD50 Classification** Class 4 in AD / Class 3 in AD / Class 4 in AD / Class 3 in AD
$C_{25}H_{38}O_6$	**Rat IP LD50 Log10(mmol/kg)** / **Rat IV LD50 log10(mmol/kg)** / **Rat Oral LD50 log10(mmol/kg)** / **Rat SC LD50 log10(mmol/kg)** -0,636 in AD / -1,449 in AD / 0,143 in AD / -1,746 in AD **Rat IP LD50 (mg/kg)** / **Rat IV LD50 (mg/kg)** / **Rat Oral LD50 (mg/kg)** / **Rat SC LD50 (mg/kg)** 100,600 in AD / 15,460 in AD / 604,000 in AD / 7,799 in AD **Acute Rodent Toxicity Classification of Chemicals by OECD Project** **Rat IP LD50 Classification** / **Rat IV LD50 Classification** / **Rat Oral LD50 Classification** / **Rat SC LD50 Classification** Class 4 in AD / Class 3 in AD / Class 4 in AD / Class 2 in AD

$C_{28}H_{27}NO_4S$ (standard)	**Rat IP LD50 Log10(mmol/kg)** | **Rat IV LD50 log10(mmol/kg)** | **Rat Oral LD50 log10(mmol/kg)** | **Rat SC LD50 log10(mmol/kg)** -0,095 in AD | -0,851 in AD | 0,433 in AD | 0,029 out of AD **Rat IP LD50 (mg/kg)** | **Rat IV LD50 (mg/kg)** | **Rat Oral LD50 (mg/kg)** | **Rat SC LD50 (mg/kg)** 380,800 in AD | 66,740 in AD | 1283,000 in AD | 505,800 out of AD **Acute Rodent Toxicity Classification of Chemicals by OECD Project** **Rat IP LD50 Classification** | **Rat IV LD50 Classification** | **Rat Oral LD50 Classification** | **Rat SC LD50 Classification** Class 4 in AD | Class 4 in AD | Class 4 in AD | Class 4 out of AD

6.4 DOCKING STUDIES:

MODE	AFFINITY OF LIGANDS WITH TARGET- BACE-1					Standard
	$C_{25}H_{34}O_6$	$C_9H_{11}ClO_2$	$C_9H_9ClO_3$	$C_{26}H_{38}O_6$	$C_{25}H_{38}O_6$	$C_{28}H_{27}NO_4S$
1	-7.6	-4.2	-4.5	-6.8	-7.1	-6.8
2	-7.1	-4.2	-4.5	-6.4	-7.1	-6.7
3	-7.0	-4.2	-4.5	-6.4	-6.9	-6.7
4	-7.0	-4.1	-4.4	-6.3	-6.6	-6.5
5	-6.9	-4.1	-4.3	-6.2	-6.6	-6.3
6	-6.9	-4.1	-4.2	-6.1	-6.6	-6.3
7	-6.9	-4.1	-4.2	-6.1	-6.5	-6.2
8	-6.8	-4.1	-4.2	-5.9	-6.4	-6.2
9	-6.8	-4.1	-4.1	-5.8	-6.3	-6.1

MODE	AFFINITY OF LIGANDS WITH TARGET- ESTROGEN RECEPTOR					Standard
	$C_{25}H_{34}O_6$	$C_9H_{11}ClO_2$	$C_9H_9ClO_3$	$C_{26}H_{38}O_6$	$C_{25}H_{38}O_6$	$C_{28}H_{27}NO_4S$
1	-7.9	-5.1	-5.3	-7.2	-9.5	-7.5
2	-7.8	-5.0	-5.1	-6.9	-8.6	-7.2
3	-7.7	-4.9	-5.1	-6.6	-6.7	-6.2
4	-7.4	-4.8	-5.1	-6.3	-6.6	-5.9
5	-7.4	-4.5	-5.0	-5.9	-6.5	-5.9
6	-7.3	-4.5	-5.0	-5.7	-6.4	-5.7
7	-7.2	-4.5	-4.9	-5.6	-6.4	-5.7
8	-7.0	-4.3	-4.4	-5.4	-6.2	-5.7
9	-6.9	-4.2	-4.4	-5.3	-6.0	-5.7

6.5 BIOVIA VISUALIZATION:
INTERACTIONS OF LIGANDS WITH TARGET BACE-1

Ligand name	Target ligand complex	2d interactions	Interactions of protein with ligand
$C_{25}H_{34}O_6$	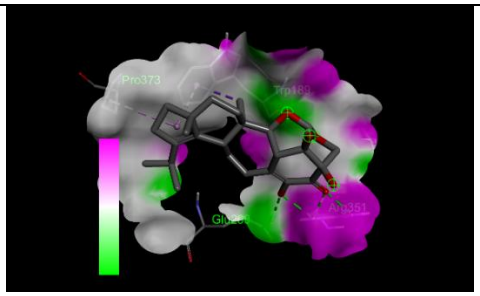	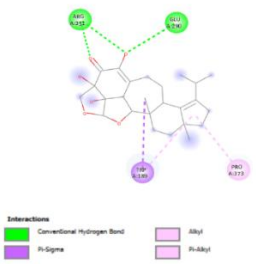	Arginine at position A:351 and Glutamic acid at position A:290 form a conventional hydrogen bonding. Tryptophan at position A:189 forms pi-alkyl and pi-sigma interactions Proline at position A:373 also forms a pi-alkyl bond

$C_9H_{11}ClO_2$	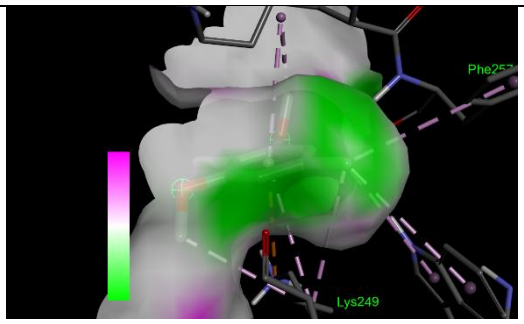	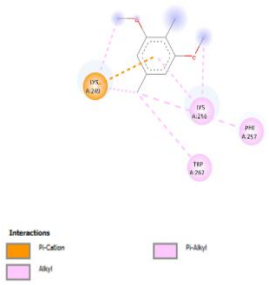	Lysine at position A:249 forms pi-cation interaction Lysine at position A:256, phenylalanine at position A:257, and tryptophan at position A:262 forms pi-alkyl interactions
$C_9H_9ClO_3$	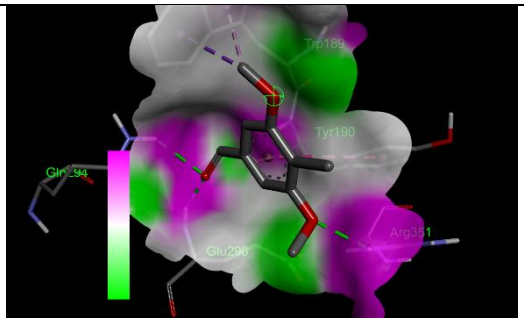	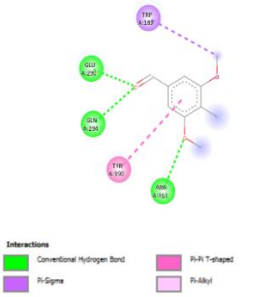	Glutamic acid at A:290, glutamine at A:294, and arginine at A:351 participate in conventional hydrogen bonding Tryptophan at A:189 forms a pi-sigma interaction Tyrosine at A:190 forms pi-pi T- shaped interactions

$C_{26}H_{38}O_6$	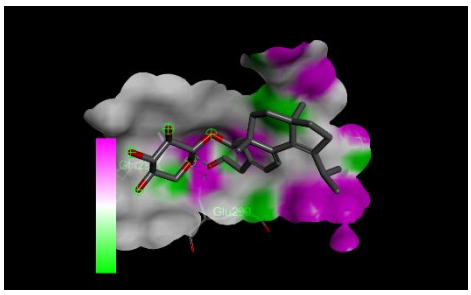	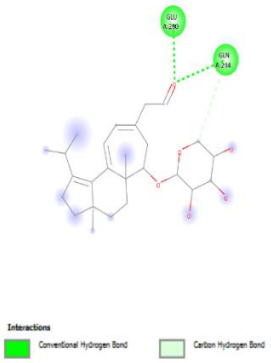	Glutamic acid at A.290 forms a conventional hydrogen bond Glutamine at A.294 forms a conventional hydrogen bond and carbon-hydrogen bonding

$C_{25}H_{38}O_6$	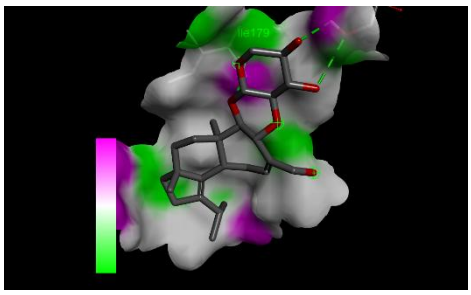	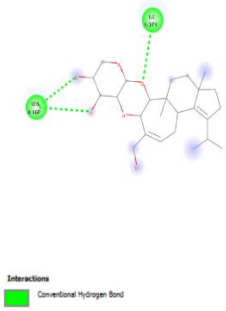	Serine at A.46P forms multiple conventional hydrogen bonds and Isoleucine at A.179 forms a single conventional hydrogen bond
$C_{28}H_{27}NO_4S$ (Standard)	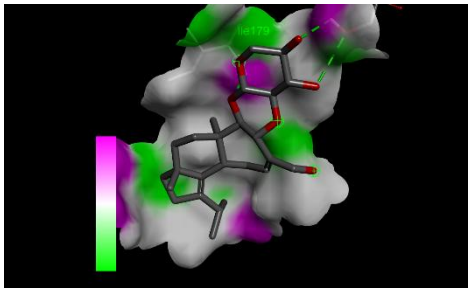	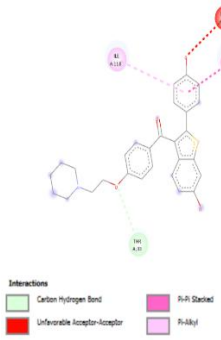	Isoleucine at A.118 forms a pi-alkyl bond Threonine at A.33 forms a carbon-hydrogen bond Tyrosine at A.114 shows unfavorable acceptor-acceptor interaction Tryptophan at A.115 forms pi-pi stacked interaction

Interactions of ligands with target Estrogen Receptor:

Ligand name	Target ligand complex	2d interactions	Interactions of protein with ligand
$C_{25}H_{34}O_6$	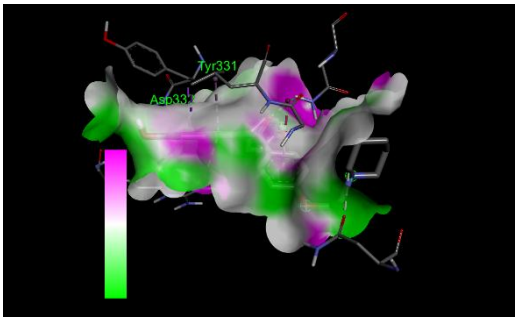	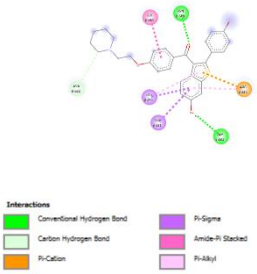	Asparagine at B:348 and aspartic acid at B:332 forms a conventional hydrogen bond, Leucine at B:345 forms pi-sigma and pi-alkyl bonds Tyrosine at B:331 makes pi-sigma bond, Arginine at B: 335 forms pi-cation and pi-alkyl bond, glycine at B: 344 forms amide pi-stacked interactions and Asparagine at B:532 show carbon hydrogen bond,

$C_9H_{11}ClO_2$	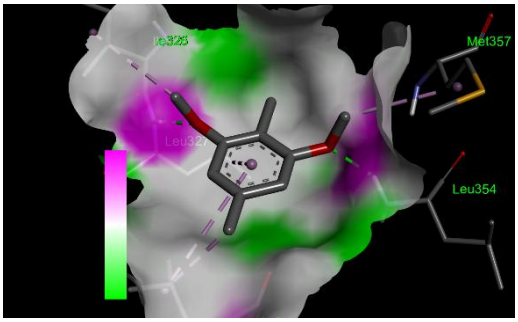	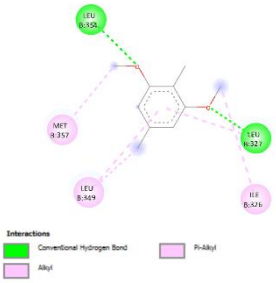	Conventional hydrogen bonds with Leucine at B: 354 and Leucine at B:327. Pi–alkyl interactions at Methionine at B:357, Leucine at position 349, Leucine at position 327, and Isoleucine at position 326.
$C_9H_9ClO_3$	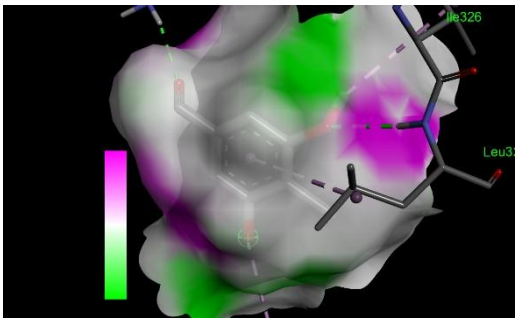	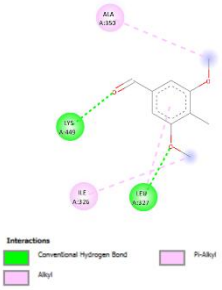	Conventional hydrogen bonds with Lysine at position 449 and Leucine at position 327, pi–alkyl interactions with Alanine at position 350, Isoleucine at position 326 , and Leucine at position 327.

$C_{26}H_{38}O_6$	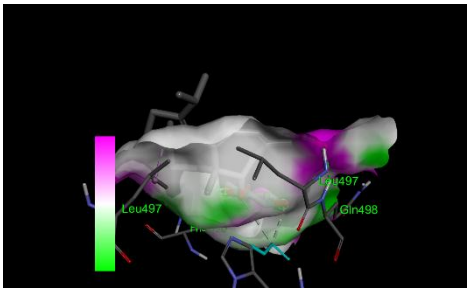	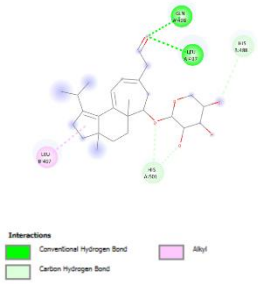	Conventional hydrogen bonds with Glutamine at position 498 and Leucine at position 497.carbon hydrogen bonding with Histidine at position 488 and Histidine at position 501. An alkyl interaction with Leucine at position 497 of chain B.

$C_{25}H_{38}O_6$	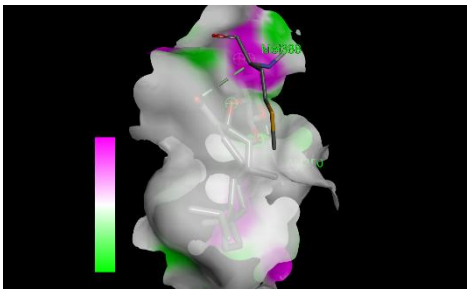	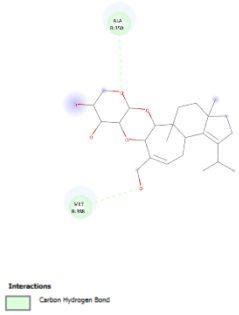	Carbon hydrogen bonds with Alanine at position 350 and Methionine at position 388.
$C_{28}H_{27}NO_4S$ (Standard)	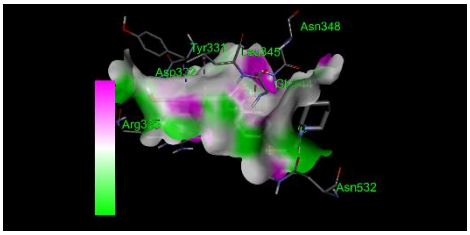	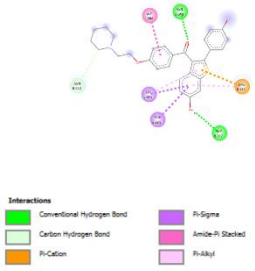	Asparagine at A:348 and aspartic acid at A: 332 form conventional hydrogen bond Asparagine at A: 532 also forms a carbon-hydrogen bond Leucine at A:345 and tyrosine at A:331 forms a pi-sigma bond Arginine at A: 335 forms a pi-cation bond Glycine at A:344 shows amide-pi-stacked interaction

VII. DISCUSSION:

This study employed computer-aided drug design (CADD) techniques to evaluate the neuroprotective potential of secondary metabolites from the *Hericium* genus against key targets in Alzheimer's Disease (AD), specifically beta-secretase (BACE1) and estrogen receptor alpha (ERα). Through in silico modelling, including ADMET analysis, toxicity prediction, and molecular docking, erinacines and related bioactives demonstrated momentous therapeutic promise. All selected compounds exhibited favourable physicochemical properties as per Lipinski's rule of five, indicating good oral bioavailability. Remarkably, no violations were observed across all test compounds. The ADME analysis revealed high gastrointestinal absorption for all ligands. In docking studies, compound $C_{25}H_{38}O_6$ exhibited the highest binding affinity with ERα (as low as −9.5 kcal/mol), surpassing the standard drug Raloxifene (−7.5 kcal/mol), suggesting a strong interaction with neuroprotective targets. Similarly, $C_{25}H_{34}O_6$ and $C_{25}H_{38}O_6$ demonstrated favourable binding with BACE1, with docking scores of −7.6 and −7.1 kcal/mol, respectively. These interactions involved critical amino acids such as Glu290, Arg351, and Trp189, which are key residues in BACE1's active site. Visual inspection of 2D interactions confirmed hydrogen bonding, pi-alkyl, and hydrophobic interactions, reinforcing the stability of ligand-target complexes. Toxicological prediction using GUSAR showed all compounds had acceptable LD50 values, implying low acute toxicity and favourable safety profiles. Collectively, these results confirm the therapeutic relevance of erinacines and other *Hericium*-derived compounds in targeting AD-related pathophysiology, especially in mitigating amyloid plaque formation and modulating estrogen receptor dysfunction.

VIII. CONCLUSION:

The present study demonstrates that bioactive compounds from the *Hericium* genus—particularly erinacines S, A, and C—possess substantial therapeutic potential in Alzheimer's disease management through dual inhibition of BACE1 and modulation of ERα. Computational predictions suggest that these molecules have excellent pharmacokinetic properties, low toxicity. Molecular docking studies established strong binding affinities with both BACE1 and ERα, supporting their role in reducing amyloid-beta accumulation and enhancing neuroprotection.

Reference:

[1] S. Surabhi and B. Singh, "Computer Aided Drug Design: an Overview," *J. Drug Deliv. Ther.*, vol. 8, no. 5, pp. 504–509, 2018, doi: 10.22270/jddt.v8i5.1894.

[2] J. QI *et al.*, "The chemical structures, biosynthesis, and biological activities of secondary metabolites from the culinary-medicinal mushrooms of the genus Hericium: a review," *Chin. J. Nat. Med.*, vol. 22, no. 8, pp. 676–698, 2024, doi: 10.1016/S1875-5364(24)60590-X.

[3] C. Y. Lin *et al.*, "Erinacine S from Hericium erinaceus mycelium promotes neuronal regeneration by inducing neurosteroids accumulation," *J. Food Drug Anal.*, vol. 31, no. 1, pp. 32–54, 2023, doi: 10.38212/2224-6614.3446.

[4] I. C. Li *et al.*, "Prevention of Early Alzheimer's Disease by Erinacine A-Enriched Hericium erinaceus Mycelia Pilot Double-Blind Placebo-Controlled Study," *Front. Aging Neurosci.*, vol. 12, no. June, pp. 1–13, 2020, doi: 10.3389/fnagi.2020.00155.

[5] I. Szućko-Kociuba, A. Trzeciak-Ryczek, P. Kupnicka, and D. Chlubek, "Neurotrophic and Neuroprotective Effects of Hericium erinaceus," *Int. J. Mol. Sci.*, vol. 24, no. 21, 2023, doi: 10.3390/ijms242115960.

[6] D. Agnusdei and N. Iori, "Raloxifene: results from the MORE study.," *J. Musculoskelet. Neuronal Interact.*, vol. 1, no. 2, pp. 127–32, 2000, [Online]. Available: http://www.ncbi.nlm.nih.gov/pubmed/15758505

[7] Z. Liu *et al.*, "Raloxifene alleviates amyloid-β-induced cytotoxicity in HT22 neuronal cells via inhibiting oligomeric and fibrillar species formation.," *J. Biochem. Mol. Toxicol.*, vol. 33, no. 11, p. e22395, Nov. 2019, doi: 10.1002/jbt.22395.

[8] T. Nohara *et al.*, "Neuroprotective Potential of Raloxifene via G-Protein-Coupled Estrogen Receptors in Aβ-Oligomer-Induced Neuronal Injury," *Biomedicines*, vol. 11, no. 8, pp. 1–19, 2023, doi: 10.3390/biomedicines11082135.

[9] G. L. Cipriano, E. Mazzon, and I. Anchesi, "Estrogen Receptors: A New Frontier in Alzheimer's Disease Therapy," *Int. J. Mol. Sci.*, vol. 25, no. 16, 2024, doi: 10.3390/ijms25169077.

[10] M. S. Uddin *et al.*, "Estrogen Signaling in Alzheimer's Disease: Molecular Insights and Therapeutic Targets for Alzheimer's Dementia.," *Mol. Neurobiol.*, vol. 57, no. 6, pp. 2654–2670, Jun. 2020, doi: 10.1007/s12035-020-01911-8.

[11] H. Hampel *et al.*, "HHS Public Access," vol. 89, no. 21, pp. 745–756, 2021, doi: 10.1016/j.biopsych.2020.02.001.The.